The effects of pH, time and temperature on the stability and viscosity of cellulose nanocrystal (CNC) dispersions – Implications for use in enhanced oil recovery

Authors: Silje N. Molnes[a,b]; Kristofer G. Paso[b]; Skule Strand[a]; Kristin Syverud[b,c,*]

[a] *Department of Petroleum Technology, University of Stavanger (UoS), 4036 Stavanger, Norway*

[b] *Department of Chemical Engineering, Norwegian University of Science and Technology (NTNU), 7491 Trondheim, Norway*

[c] *Paper and Fibre Research Institute (PFI), Høgskoleringen 6B, 7491 Trondheim, Norway*

*Corresponding author.
E-mail address: kristin.syverud@pfi.no (K. Syverud)
Phone: +47 959 03 740

Key words:
Nanocellulose
Stability
Oil recovery
CNC
Temperature
Heat aging

Abstract

Cellulose nanocrystals (CNC) are currently being investigated as potential additives for enhanced oil recovery (EOR). Presented in this paper is a study investigating the effects of different physical and chemical environments that low concentration CNC dispersions may be subjected to at oil reservoir conditions. Different concentrations of CNC dispersed in de-ionized water and in a 1000 ppm NaCl brine were subjected to variations in pH and temperature, and the results showed that the dispersions remained stable in the pH range expected in oil reservoirs (between 5 and 9). Stable dispersions were also observed when heated to temperatures ranging from 50 to 90 °C. At extended heat aging at 90 °C and 120 °C for seven days; beginning degradation was observed for both types of CNC dispersions; with viscosity increase and pH decrease as the most important indicators. CNC dispersed in 1000 ppm NaCl brine was generally more heat tolerant than the CNC dispersed in de-ionized water. The increase in viscosity during heat aging can be very interesting for enhanced oil recovery applications. A fluid that increases its viscosity with heat and time will be easier to inject due to a low initial viscosity, and when the viscosity increases in the porous reservoir, the effect can be a stable waterfront and less viscous fingering, which again can lead to increased sweep efficiency and better oil recovery.

1. Introduction

Cellulose is the most abundant naturally occurring biomaterial on Earth. It is most commonly found in the wall of plant cells, where it provides stiffness and structure, but it is also found in marine animals, like tunicates, as well as bacteria, fungi and algae (Habibi et al., 2010). The

biopolymer was first isolated and described by Anselme Payen in 1838 (Payen, 1838), and has since been the subject of numerous studies, with new aspects still being discovered.

Nanocelluloses are products derived from cellulose, which have at least one dimension in the nanometre range. They are produced via various chemical and mechanical processes, and are used for an ever-increasing number of applications, depending on their physical properties. One such type of nanocellulose is cellulose nanocrystals (CNC), which is the smallest cellulose fragment available today. CNC have diameters typically ranging from 5 – 70 nm, and lengths from 100 – 250 nm when hydrolysed from plant celluloses, and 100 nm to several microns when produced from bacteria and tunicates (Klemm et al., 2011). Colloidal suspensions of CNC produced by acid hydrolysis was first reported in 1949 (Rånby, 1949).

Acid hydrolysis is the most commonly used production pathway for CNC, and in this process the amorphous regions of the cellulose fibril are removed, while the more acid-resistant crystalline regions remain intact (Beck-Candanedo et al., 2005). There are two main approaches when using mineral acid hydrolysis; the use of HCl, or the use of H_2SO_4, which gives the resulting CNC slightly different properties. CNC hydrolysed with HCl will have better thermal properties than CNC prepared with H_2SO_4, but the latter will have better dispersability in polar solvents like water (Camarero Espinosa et al., 2013).

Which characteristics do these particles exhibit when exposed to elevated temperatures and fluctuations in pH values? Extensive research has been performed on the temperature stability of CNC, and it has been found that CNC is being degraded when subjected to temperatures above 220 °C (Chen et al., 2016). It should be noted that these values for CNC are acquired through thermogravimetric analysis (TGA), which is performed on dried CNC in an inert atmosphere of N_2 gas (N. Wang et al., 2007). For aqueous dispersions, the situation, as well as degradation temperature, will be different. This topic has recently

been addressed by Heggset et al., through the assessment of degradation products from different nanocellulose products, aged at high temperatures as aqueous dispersions (Heggset et al., 2017).

The question about the stability of aqueous CNC dispersions is relevant due to the ongoing investigations of CNC as a potential new additive for enhanced oil recovery (EOR). When applied in an oil reservoir, dispersed CNC will meet shear forces, changes in water chemistry and elevated temperatures. Reservoir temperature rises with increasing depth, or closeness to the Earth's mantle. This varies with the geothermal gradient, but a general rule of thumb is that the temperature is increased with 3 °C per 100 m depth, with temperatures reaching above 150 °C (Beal, 1946; Jahn et al., 2008). The reservoir mineralogy affects the flooding brine chemistry, and it has been experimentally observed in core experiments at reservoir conditions that a slightly acidic CNC dispersion increased its pH after being flooded through a sandstone core (Molnes et al., 2016). At acidic conditions, cellulose may be cleaved through a hydrolysis reaction at the 1-4 glycosidic bond (Battista, 1950), but as the pH values in sandstone reservoirs typically varies between 6 and 9, acid hydrolysis will (probably) not be the major pathway of CNC degradation. Cellulose derivatives have been shown to degrade very slowly under alkali conditions, but for this situation to occur, the temperature have to be above 170 °C (Wellington, 1983). Thus, the most likely pathway for CNC degradation below 150 °C in an oil reservoir would be through radical, oxidative/reductive depolymerisation (ORD). In such a reaction, a free radical containing one or more unpaired electrons can attack polymers, causing depolymerisation. Biopolymers are especially vulnerable to autoxidation, where H_2O_2 radicals are formed, leading to propagating chain reactions (Heggset et al., 2017; Wellington, 1983).

During core flooding and recovery experiments in the laboratory, the CNC crystallite dispersions can be subjected to high temperatures, shear forces, variations in pH and dispersion/brine chemistry, as well as pressure, in an effort to mimic the conditions in an actual oil reservoir. It is therefore of great interest to map how the CNC dispersions responds to these changes, as it is a good predictor to how the material will behave in action in a reservoir, which is why this is the main scope of this research article. The salt stability of CNC in LS brine has earlier been investigated (Boluk et al., 2011; Molnes et al., 2016), and CNC has been deemed stable within the salt concentrations used for this application. When performing experiments on sandstone cores, it is important that the flooding brine is of a saline nature. If the salinity of the pore water decreases, the clays in the core material may start to swell, which again will destroy the permeability of the core, making particle flooding difficult/impossible (Gray & Rex, 1965).

In this study, CNC dispersions have been subjected to pH values and temperatures they are expected to encounter during core flooding and oil recovery experiments. To evaluate the effect of the treatment, the viscosity and colloidal stability of the dispersions have been tested. Atomic force microscopy (AFM) have also been utilised to examine the heat-aged particles visually.

2. Materials and Methods

Concentrated stock dispersion (11.8 wt. % in DI-water) of CNC was purchased from the University of Maine. It was produced by the US Forest Service's Forest Products Laboratory

(Madison, Wisconsin), by using sulphuric acid (64 %) hydrolysis to remove the amorphous sequences of the material. This procedure leaves crystalline, rod-like particles with a net negative charge due to sulphate half ester groups produced on the surface of the CNC particles during the hydrolysis reaction (Abitbol et al., 2013). Crystallites from the same batch were analysed by Heggset et al. (2017), and the most important characteristics are given in Table 2.1.

Table 2.1: CNC characteristics, adapted from (Heggset et al., 2017) and (Sacui et al., 2014).

Sample	Charge density (mmol/g)	Crystallite diameter (nm)[c]	Crystallite length (nm)[c]	Functional groups
CNC	approx. 0.3[a, b]	5.9 ± 1.8	130 ± 67	-OH, -SO_3H

[a]Amount of sulphate ester groups
[b]Measured with inductively coupled plasma-atomic absorption (ICP-AA) (Heggset et al., 2017).
[c]Determined with atomic force microscopy (AFM) (Sacui et al., 2014).

The samples were prepared by dilution to desired concentrations (in wt. %) with either de-ionized water (DI-water, 18.2 mΩ), or with 1000 ppm NaCl brine, (low salinity/LS brine). The LS brine was prepared by stirring reagent grade NaCl (Sigma-Aldrich) and DI-water, before filtration over a 0.22 µm Millipore filter using a vacuum pump, to remove impurities. Samples were stored in refrigerator if needed. The dispersions will from now on be denoted CNC-DI and CNC-LS, respectively.

pH was measured using a Mettler Toledo SevenCompact pH-meter (Mettler-Toledo International Inc., Columbus, OH, USA) and sonication procedures were performed using a VWR Ultrasonic Cleaner (VWR International, Radnor, PA, USA).

2.1 Rheology

For the rheology measurements, an Anton Paar MCR 301 rotational rheometer fitted with different types of measurement configurations was used. Three different types of viscosity-related experiments were performed. All sample dispersions were prepared from the 11.8 wt. % CNC stock dispersion. All tests were run using the Rheoplus software, v3.40.

Dispersion viscosities at varying pH

40 mL samples of 0.5 wt. % were prepared by using 1.7 mL stock dispersion with either 38.3 mL DI water or 38.3 mL LS brine. The pH was adjusted to the desired value by titration with either 50 mM NaOH or 50 mM HCl, both prepared from laboratory grade reagents and DI water. Table 2.2 shows the pH values of the samples before and after titration.

Table 2.2: pH values for the tested samples, before and after titration with either 50 mM NaOH or 50 mM HCl.

Sample type	Initial pH	Desired pH	Testing pH
CNC-DI	6.9	5	5.1
CNC-DI	7.1	6	6.1
CNC-DI	7.1	7	6.9
CNC-DI	7.3	8	7.9
CNC-DI	7.0	9	8.9
CNC-LS	5.6	5	5.2
CNC-LS	5.7	6	6.0
CNC-LS	5.7	7	7.0
CNC-LS	5.7	8	8.1
CNC-LS	5.7	9	9.0

Each sample was sonicated for 5 minutes before rheology measurements. The rheometer was fitted with a 1° cone and plate geometry, with a 50 mm diameter cone. The shear rate was set from 10 to 1000 1/s, and the tests were performed at 20 °C.

Heat aging

The first experiment was performed to investigate how the shear viscosity of 2.0 wt. % CNC dispersions in either DI water or LS brine was affected by aging at 120 °C. Eight Schott bottles, four with 2.0 wt. % CNC-DI and four with 2.0 wt. % CNC-LS, were equipped with heat resistant lids and filled with respective dispersions. Six of the bottles were put into a heating cabinet at 120 °C. The shear viscosity of the two non-aged dispersions was measured immediately using a 2°, 50 mm diameter cone and plate geometry, with shear rates ranging from 0.1 – 1000 1/s. All measurements were performed at 20 °C. The rest of the bottles were left in the heating cabinet for 24, 48 and 168 hours, respectively. After cooling down, they were subjected to similar measurements as the non-stored samples. A simplified overview of the working flow is shown in Figure 2.1.

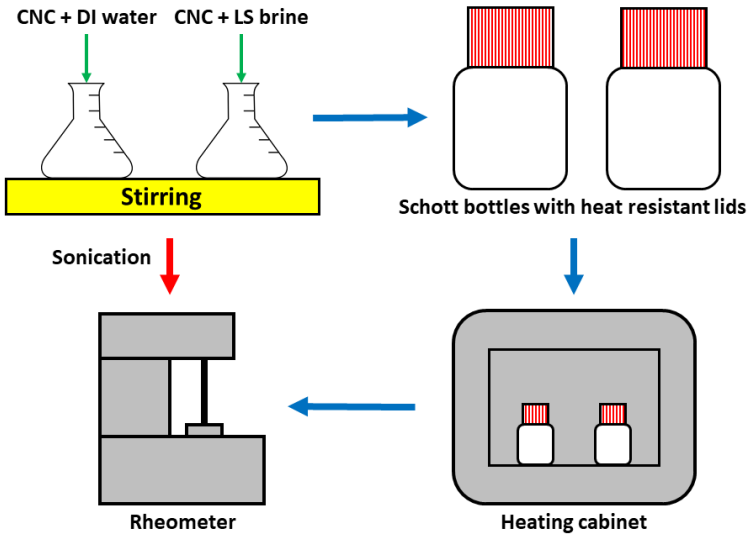

Figure 2.1: Overview of sample preparation, heat aging and testing of the CNC samples. The blue arrows indicate the work flow for heat aging in storage, and the red arrow indicates the flow for the continuous heat aging.

Continuous aging and viscosity measurements

For the continuous viscosity measurements, a CC27 cylinder and cup geometry was used. The samples were sonicated, as indicated in Figure 2.1, for 5 minutes before starting the experiments, to rid the dispersion of agglomerates. A thin layer of low viscosity silicon oil (Brookfield Viscosity Standard 9.4 cP, Marlboro, MA, USA) was used to cover the samples during the measurements, to prevent water evaporation from the sample cup. The experiment was set up with a parameter file running for 25 hours and 10 minutes. After an initial 4 min sample equilibration interval, two types of alternating intervals were used; 15 minutes long shear intervals using a shear rate of 50 1/s, and 120 minutes long "hold" intervals, where the cylinder was kept immobile in the cup. Measurement points were only taken out during the shear measurements. Everything was performed at 90 °C. The parameter file was restarted exactly at 25 hours and 10 minutes. The first 6 experiments were performed in three parallels each, for a total of 50 hours and 20 minutes. These experiments were

performed on 2.0 wt. % CNC-DI and CNC-LS. For the two last measurements, the total measuring time was extended to 175 hours. These tests were performed on 0.5 and 2.0 wt. % CNC-LS.

2.2 Zeta potential measurements

The zeta potential measurements were performed using a Malvern Zetasizer Nano ZS (Malvern Instruments Ltd, Malvern, Worcestershire, UK). The instrument determines the zeta potential through a combination of laser Doppler velocimetry (LDV) and electrophoresis, by using the Smoluchowski approximation.

For the pH dependency measurements, a Malvern MPT-2 autotitrator equipped with a pH probe and 0.05 M NaOH and HCl titrants was utilized. The titrants were prepared by using reagent grade chemicals and DI water. The experiment was performed at room temperature, and therefore the standard folded capillary cell (DTS1070) was utilized. For the experiment using temperatures from 50 – 90 °C, a dip cell kit equipped with a quartz cuvette was used, as the DTS1070 is damaged by higher temperatures. All experiments were performed on 0.5 wt. % dispersions, prepared with either DI water or LS brine.

2.3 Atomic Force Microscopy

Images of dispersed CNC were aquired by atomic force microscopy (AFM), using a Bruker Multimode V AFM with a Nanoscope V Controller (Veeco Instruments Inc., Santa Barbara, CA, USA). The operation mode used was quantitative nanomechanical mapping (QNM) with

automated settings, and the images were acquired using the Scan Asyst mode in air at ambient temperature. AFM tips were provided by Bruker AFM Probes (Bruker Nano Inc., Camarillo, CA, USA). These probes have a silicon tip on a nitride lever, and a spring constant of 0.4 N/m. The image area was varied between 5 x 5 and 1 x 1 µm, and the resolution was either 512 or 1024 pixels per line. Scans were analysed using NanoScope Analysis v1.40, and modified with ImageJ v1.50i.

The samples were prepared according to the method used by (Lahiji et al., 2010). A drop of CNC dispersion (~0.5 and ~2.0 wt. %) was placed on freshly cleaved 10 mm mica disks (Agar Scientific Ltd., Essex, UK), glued to magnetic sample holders. The drop was left on the mica for 1 minute, before the surface was rinsed using DI water and dried using compressed N_2 gas. This method provides strong-adhering CNC particles that are well dispersed on the mica surface.

3. Results and Discussion

3.1 Zeta potential measurements

CNC in dispersion is stabilised through the electrical double layer (EDL) that exists between the particles due to the negatively charged sulphate ester groups that are formed on the CNC surface during acid hydrolysis (Dong et al., 1996). This causes a certain concentration-dependent viscosity, which can be lowered by increasing the ionic strength of the dispersing medium (Boluk et al., 2011), or by subjecting the crystallites to extreme chemical conditions. A method for assessing the stability of dispersed particles is to measure the zeta potential. This parameter is associated with the electrokinetic properties of a particle in dispersion

(Leong & Ong, 2003; Sarkar & Nicholson, 1996; S. C. Wang & Wei, 2001; Will et al., 2001). A dispersion is deemed stable if the zeta potential is above ± 30 mV (Salopek et al., 1992).

When injection brines are flooded through a sandstone medium, the pH might fluctuate between ~5 and ~9. It was therefore of interest to investigate the change in colloidal stability of the CNC dispersions within this pH range. Zeta potential experiments were performed at 20 °C on 0.5 wt. % CNC dispersed in both DI water and 1000 ppm NaCl. The pH of the dispersions was varied between 5 and 9 using an autotitrator, and the results are shown in Figure 3.1.

a)

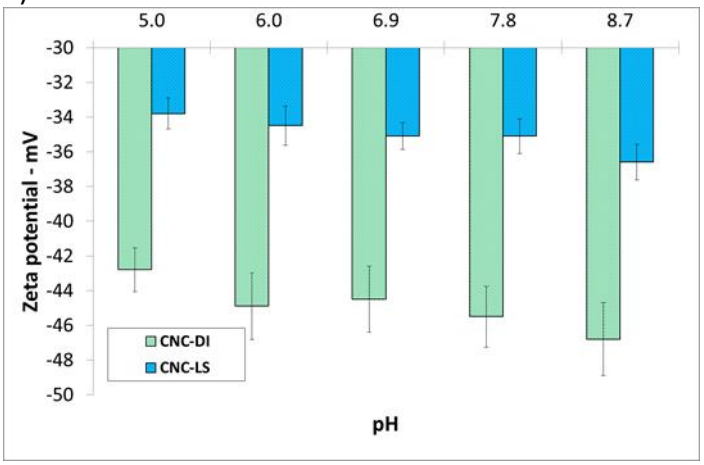

b)

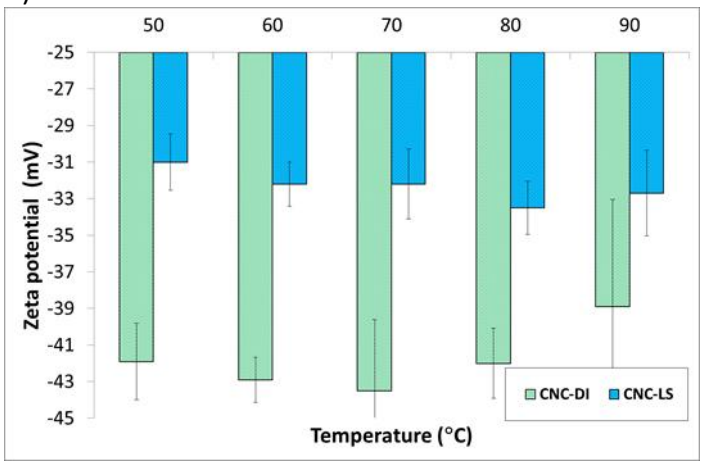

Figure 3.1 a) Zeta potential as an effect of pH, and b) zeta potential as an effect of increasing temperature.

Present observations show that the zeta potential is negative for all the tested dispersions, due to the negatively charged sulphate ester groups formed on the CNC surface during production. Results obtained were expected and in accordance with earlier observations (Molnes et al., 2016). The zeta potential for the CNC dispersed with low saline brine varied between -33.8 ± 0.9 mV at pH 5 to -36.6 ± 1.0 at pH 9, which was lower than that of the CNC dispersed with DI water, which varied between -42.8 ± 1.3 mV and -46.8 ± 2.1 mV for the same pH values. This effect is caused by sodium ions shielding the negatively charged sulphate esters on the CNC surface, which causes the electrostatic double layer (EDL) to shrink,

allowing the particles to move closer together, which again causes a reduction in the zeta potential. As can be seen in the figure, the zeta potential stayed below the limit where a dispersion is regarded stable (above 30 mV in absolute value, Salopek et al., 1992), for all pH values tested, in both type of dispersions, and that the negativity remained almost constant with increasing pH, indicating that the isoelectric point (IEP) may be lower than pH 5. From this it can be deduced that no significant effect of pH was observed within the tested range, and aqueous dispersions of CNC will remain stable within the pH values that are encountered in the lab scale sandstone oil reservoir used previously.

Zeta potential values were also investigated for CNC dispersions at increasing temperatures, ranging from 50 – 90 °C. Dispersion pH was measured before the experiments, and it was 6.3 for the CNC-DI dispersion, and 5.5 for the CNC-LS dispersion. The results are shown in Figure 3.1, and reveals that there are no significant differences between the zeta potential values for the different temperatures for neither CNC-DI nor CNC-LS. Both dispersions remained within the stable limits for all the tested temperatures.

3.2 Rheology measurements

Shear viscosity tests were performed on 0.5 wt. % dispersions with pH ranging from 5 to 9, to see if the dispersion viscosity could be affected by the sandstone reservoir pH conditions. The 0.5 wt. % CNC concentration was investigated because this was the concentration that provided the best injectivity in previously performed sandstone coreflooding studies (Molnes et al., 2016). Dispersion pH was adjusted, but the volumes added were so small that it didn't affect the CNC concentration in the dispersions significantly. The results revealed that the viscosity of the dispersions did not change significantly for the pH range tested. The viscosity

of the CNC-LS samples was a bit lower than that of the CNC-DI samples. At a shear rate of 20 1/s, the viscosity was ~1.2 mPa·s for CNC-LS and ~1.5 mPa·s for CNC-DI. This is caused by the same shielding effect mentioned in the last section, where the shielding of negative charges causes shrinkage of the EDL around the CNC rods, which lowers the viscosity. In general CNC is not very sensitive to fluctuations in pH, which is also a well-known property of the parent cellulose polymer, and neither zeta potential nor viscosity is affected by changes in pH between 5 and 9. For CNC, this may be due to the relatively low charge density of the crystallite, with only 0.3 mmol/g of sulphate ester groups on the surface. The particles would probably be more pH sensitive if the charge density was higher. At higher charge densities, the rheological behaviour would also be different, and the dispersions would be more susceptible to agglomeration in response to fluctuation in electrolyte concentration.

Heat aging of CNC samples at 120 °C for 24, 48 and 168 hours

Dispersions of 2.0 wt. % CNC-DI and CNC-LS were poured into Schott bottles and placed in a heating cabinet at 120 °C. One set of bottles were tested right away, by pH and viscosity measurements, as well as visual inspection. A set of samples of both CNC-DI and CNC-LS were also heat aged at 90 °C for 168 hours. The aged dispersions were rheologically tested at 20 °C after exactly 24 hours, 48 hours and 1 week (168 hours). Shown in Figures 3.2a-d is the colour development of the 120 °C heat aged dispersions.

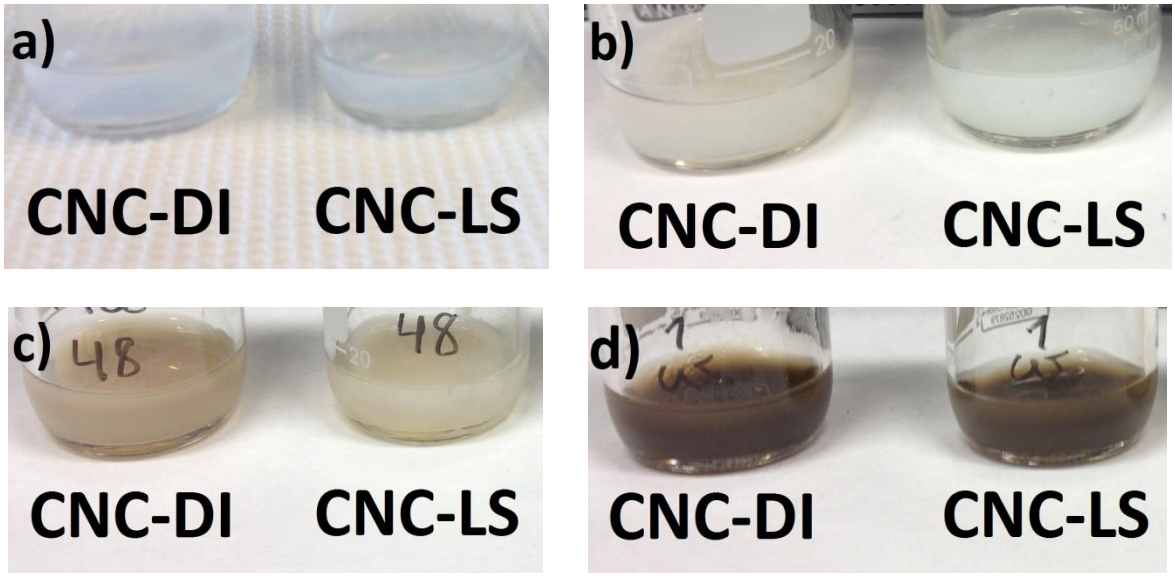

Figure 3.2 a) CNC-DI and CNC-LS dispersions right after sample preparation (t = 0). b) Samples photographed after 24 hours of heat aging at 120 °C. CNC-DI is slightly darker than CNC-LS. c) Dispersion samples after 48 hours of heat aging at 120 °C. The CNC-DI sample is still more miscoloured than the CNC-LS sample. d) After 1 week (168 hours of heat aging at 120 °C) it was not possible to distinguish between the samples, due to heavy discolouration in both samples.

As observed in Figure 3.2a-d, the dispersions showed discolouration with time, and the CNC-DI samples discoloured slightly faster than the CNC-LS samples. The samples aged at 90 °C did not show any significant colour change. Change in colour is a sign of carbohydrate degradation, and is an important parameter to include when assessing carbohydrate stability. The degradation mechanism leading to the colour change has not been thoroughly clarified yet (Matsuo et al., 2012), but a probable candidate is thermal oxidation, which occurs due to presence of oxygen. This reaction forms both aldehyde and carboxyl groups, and formation of carbonyl groups within the cellulose chains might be the cause of the very clear colour change with time and temperature (Łojewska et al., 2007; Yatagai & Zeronian, 1994). As CNC is derived from wood, the material might contain small amounts of pentose in addition to hexose monomers. The pentoses and hexoses are known to degrade through hydrolysis into furfural and hydroxymethylfurural (HMF) respectively, when being subjected to heat and acids (Dunlop, 1948). The concentration of HMF/furfural can be determined through UV-vis

spectroscopy, as they both have an absorbance spectrum of 277 nm. UV-vis was performed by Heggset et al. (2017) on CNC from the same production batch as the ones used in this article, heat aged at 140 °C for three days. They found a HMF/furfural concentration of 1 mg/L, which was substantially lower than the values for the other carbohydrate polymers tested in the article. The low HMF/furfural value was connected to the crystalline nature of CNC, making it degradation resistant (Heggset et al., 2017). Mechanisms of cellulose degradation into HMF and furfural has been suggested by (Shen et al., 2013).

The pH of the samples was also measured for each time-step, and is given in Table 3.1 and 3.2.

Table 3.1: pH change over time for 2.0 wt. % CNC dispersions aged at 120 °C**.**

Sample	pH t = 0 hours	pH t = 24 hours	pH t = 48 hours	pH t = 168 hours	Δ pH (168 h)	H^+ formed per 1000 glucose units (120 °C, 24 hrs)
CNC-DI	6.2	2.0	2.1	2.0	4.2	83
CNC-LS	5.3	2.1	2.1	2.0	3.3	83

Table 3.2: pH change over 168 hours for 2.0 wt. % CNC dispersions aged at 90 °C**.**

Sample	pH t = 0 hours	pH t = 168 hours	Δ pH (168 h)	H^+ formed per 1000 glucose units (90 °C, 168 hrs)
CNC-DI	6.6	2.7	3.9	17
CNC-LS	5.8	3.1	2.7	7

The pH of the CNC-LS samples started out lower than the CNC-DI samples. This effect has been observed earlier, and a hypothesis is that it is caused by sodium ions exchanging

hydrogen ions as co-ions to the sulphate ester groups, so the pH in the dispersion decreases as H^+-ions are being released into the dispersing medium (Molnes et al., 2016). All sample types experienced a decrease in pH, and calculated as the amount of H^+ released per 1000 glucose units, this number was the same for both samples aged at 120 °C, but substantially lower for the samples aged at 90 °C as expected. For the samples aged at 120 °C, this effect was observed already after 24 hours, and there were almost no changes during the rest of the testing period. As mentioned, during the degradation process carboxyl groups are formed through both oxidation and hydrolysis reactions on the material, and this is probably the cause of the reduction in pH. Change in pH can thus also be used as an indicator for temperature degradation of CNC. Similar results for both pH and colour change was obtained in an earlier study (Heggset et al., 2017), and thus supports this view. In the Heggset et al. article, the number of H^+ units formed in ‰ of glucose units at 140 °C was estimated to be 400. The release of H^+ can be caused by desulphation of the CNC. Released sulphuric acid can act in two different ways to catalyse the removal of ring hydroxyl groups; either by directly catalyse the removal of water, or by esterification of the surface hydroxyl groups of the CNC, which again will remove more sulphuric acid (Julien et al., 1993; Roman & Winter, 2004).

Further on, the samples were tested rheologically at 20 °C by using increasing shear rates and a 2 ° cone and plate setup. These results are shown in Figure 3.3.

357

a) b)

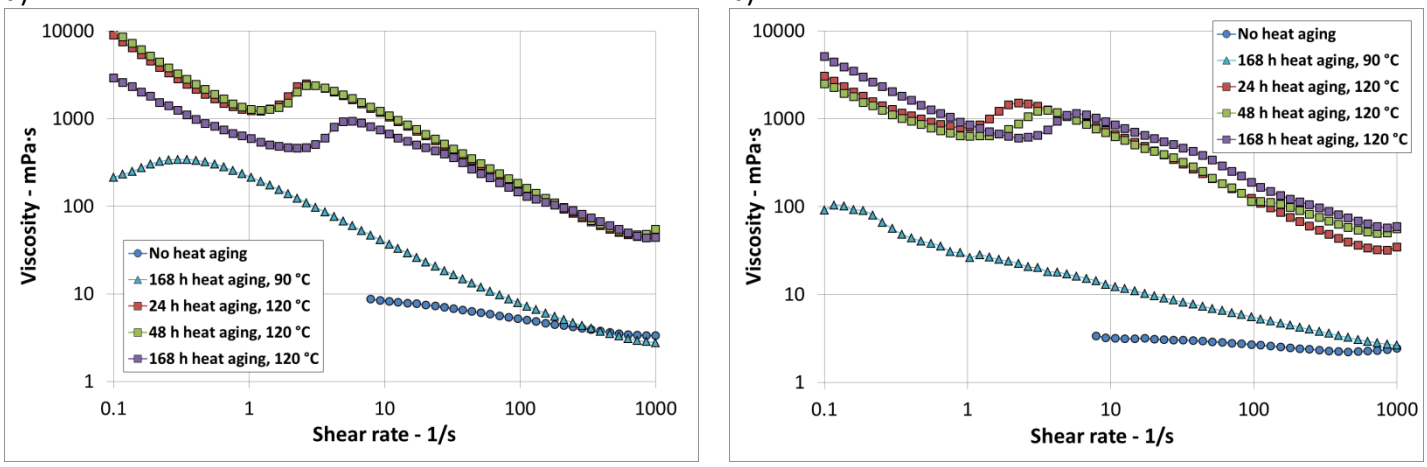

Figure 3.3: Viscosity measurements of a) CNC-DI and b) CNC-LS, performed at 20 °C on 2.0 wt. % samples after heat aging at different temperatures.

358

359 As seen in Figure 3.3, the shear viscosity profile of both the sample types increased drastically
360 after only 24 hours aging at 120 °C. The viscosity profile remained stable after aging for 168
361 hours at high temperature. As can also be seen in the figure, the CNC-LS sample that was aged
362 for the longest time at 120 °C, was also the one that showed the highest viscosity. The
363 increase in viscosity may be caused by some kind of delamination of the CNC crystallites,
364 which increases the surface area of the particles, and exposes more hydroxyl groups to the
365 surrounding medium, causing an increase in viscosity. The heat aged dispersions also showed
366 the typical rheological behaviour for liquid crystalline polymers in dispersion, with viscosity
367 profiles displaying three distinct regions of flow. These flow regions have been investigated
368 earlier using small angle neutron scattering (SANS) (Orts et al., 1998). The first region is at
369 very low shear rate, where a shear thinning is observed due to flow of particle domains. At
370 intermediate shear, these domains are broken up and the flow curve exhibits a plateau. When
371 the shear rate is increased further the individual rods in the dispersion are aligned and start
372 to flow, leading to a secondary shear thinning behaviour. For the measurements shown in
373 Figure 3.3, the first region is observed at shear rates from 0.1 to 1.0 1/s, before the plateau

region forms between 1.0 and 10 1/s. The last shear thinning region is observed from 10 to 1000 1/s, in accordance with earlier observations (de Souza Lima & Borsali, 2004; Marchessault et al., 1961). The viscosity profiles for the samples aged at 90 °C for 168 hours (also shown in Figure 3.3) showed a generally lower viscosity, and did not distinctly display the three before mentioned shear regions, although the overall profile was shear thinning. These results indicate that a certain temperature and aging period is required to obtain this dramatic increase in shear viscosity. This effect might be beneficial in an EOR perspective, as increased temperature and particle retention in the oil reservoir may lead to the same viscosity increase in the dispersions. This can reduce viscous fingering of the waterfront, as well as promote microscopic flow diversions through a log-jamming mechanism in the pore throats (Skauge et al., 2010), and thus lead to better tertiary oil recovery.

Dynamic time and temperature

To investigate the effect of the sodium chloride and increased viscosity with time and temperature, the samples were subjected to a shear-rest regimen combined with heat aging, using the rotational rheometer as described in Section 2.1. First, the samples were tested for 50 hours at 90 °C, and the results are shown in Figure 3.4a and b.

a)

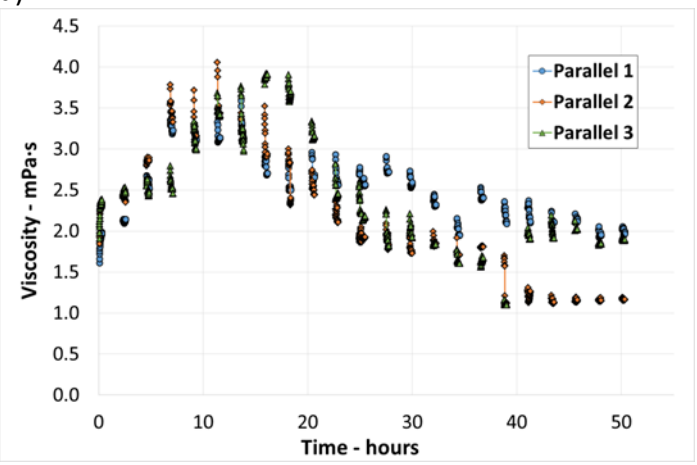

b)

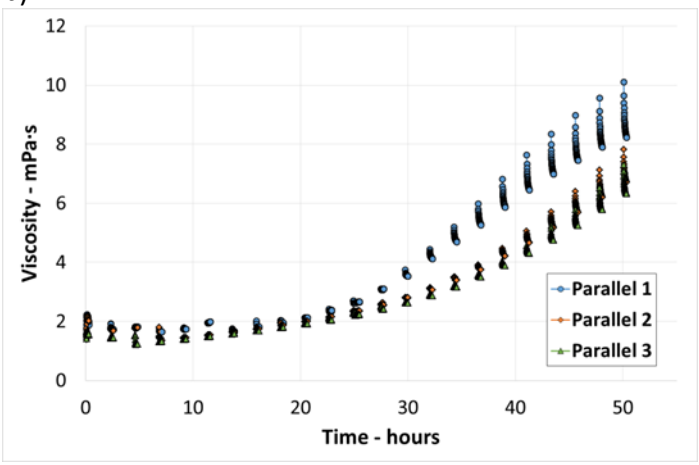

Figure 3.4: a) Viscosity development for a) 2.0 wt. % CNC-DI dispersion, and b) 2.0 wt. % CNC-LS dispersion, tested at 90 °C. Each point is one viscosity measurement and was performed for 15 minutes at 50 1/s, and between each such measurement the sample was rested for 120 minutes.

As can be seen for the CNC-DI, the viscosity increases quite rapidly for approximately 10 hours, before declining gradually when approaching 50 hours of run-time. A decrease in viscosity is a sign of particle degradation, where the polymer chains are hydrolysed into single molecules, due to the mechanisms mentioned earlier. The pH also decreased (shown in Table 3.3), which might be an indication of elimination of sulphate groups from the particle surfaces, which can further lead to crystallite degradation. The amount of H^+ released per 1000 glucose monomers was low and relatively similar for the two samples.

Table 3.3: Change in pH for 2.0 wt. % CNC-DI and CNC-LS tested at 90 °C.

Sample	pH t = 0 hours	pH t = 50 hours	Δ pH	H^+ formed per 1000 glucose units (90 °C)
CNC-DI	6.4	5.0	1.4	0.1
CNC-LS	5.4	4.7	0.7	0.1

When comparing the formed H^+ per 1000 glucose units for the samples tested at 90 °C and 120 °C, it is interesting to observe that there is such a large difference in released hydrogen

412 ions. At 90 °C, only ~0.1 H^+ is formed per 1000 glucose monomers, while at 120 °C, the number
413 is 83. When the temperature is increased to 140 °C, 400 ‰ H^+ is formed (Heggset et al., 2017).
414 According to these results, the lower temperature limit for sulphate half ester cleavage would
415 be in the 90 – 120 °C range. The relatively high temperature is probably the main cause
416 leading to the before mentioned degradation processes, as the shear rate used in the
417 experiment (50 1/s) was rather low. The shear rate in a reservoir flooding with a standard
418 flow rate of 4 pore volumes per day would be even lower, so shear degradation should
419 generally not be a problem for the crystallites in question.

420 An interesting effect was seen for the CNC-LS dispersions in Figure 3.6. It can be
421 observed from the figure that the viscosity continued to increase right up to the 50 hours
422 mark. The measurements were also much more coherent, and the samples displayed a
423 thixotropic behaviour while under shear. The increase in viscosity is probably a side effect of
424 a gradual degradation of the crystallites, or breaking of agglomerates due to shear, leading to
425 an increase in surface area, which is compatible with increase in viscosity.

426 For the next step, two experiments were performed to investigate how long time it
427 would take to bring the CNC-LS samples towards viscosity loss, as was observed for the CNC-
428 DI samples already after 50 hours at 90 °C (Figure 3.4a). 0.5 and 2.0 wt. % samples of CNC-LS
429 were subjected to 175 hours of the aging regime, with alternating 15 minutes of shear at 50
430 1/s and 120 minutes of no shear, and the results are shown in Figure 3.5.
431

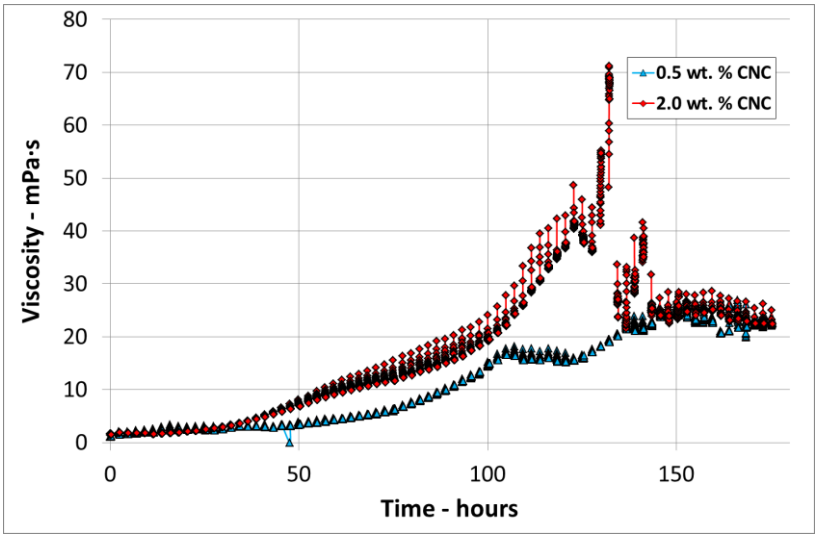

Figure 3.5: Long time heat aging experiment for 0.5 and 2.0 wt. % CNC-LS measured at 90 °C.

As can be seen in the figure, the viscosity increased steadily with time for both the tested concentrations, and the results showed the same trend as the experiment performed for only 50 hours. The viscosity of the 2.0 wt. % sample increased until the top viscosity peak at around 130 hours, before the viscosity started to decrease. The viscosity development of the 0.5 wt. % sample was slightly lower, due to the lower CNC concentration. For this measurement, the viscosity increased until around 150 hours of run-time. Both samples saw a fall in pH value, as shown in Table 3.4.

Table 3.4: pH changes for the long-term shear-rest measurements.

Sample	pH t = 0 hours	pH t = 175 hours	Δ pH	H^+ formed in ‰ of glucose units (90 °C)
0.5 wt. % CNC-LS	5.4	4.7	0.6	0.5
2.0 wt. % CNC-LS	5.5	4.4	1.1	0.3

The decrease in pH is, as mentioned, probably due to sulphuric acid released from the surface of the CNC at elevated temperatures, leading to self-catalysed depolymerisation (Roman & Winter, 2004). When the CNC starts to delaminate, the surface area of the dispersed particles

will increase, thus leading to an increase in viscosity up to a certain point were the material is broken down to such an extent that the viscosity building effect is lost.

The reason why the brines containing NaCl shows better long term temperature stability than the brines with DI water can be caused by the existence of chloride ions (Cl^-) in the dispersion. Cl^--ions are known to create competition between hydroxyl radicals and organic matter, as shown in Equations 3.1 and 3.2. This leads to inhibition of oxidation reactions, which is one of the proposed degradation routes for CNC.

$$\cdot OH + Cl^- \leftrightarrow HOCl^{-\cdot} \quad (3.1)$$

$$HOCl^{-\cdot} + H^+ \rightarrow Cl\cdot + H_2O \quad (3.2)$$

The chloride ions may also interact with the hydroxyl radicals, and in that way compete with the organic material for the radical compounds, and thus slow down the oxidation rate of the dispersed CNC. Chloride ions are thus preventing CNC degradation both through complexion and radical scavenging (Liao et al., 2001; Lu et al., 2005).

3.3 Crystallite characterization by atomic force microscopy

To investigate the effects of the heat aging, atomic force microscopy was used to image the crystallites, both before and after the heat treatment. The images are shown in Figure 3.6 and 3.7. The first image (Figure 3.6) was taken to create a reference, depicting non-aged CNC crystallites dispersed in DI water. As seen in the figure, the crystallites are slightly rounded and intact, although they show some aggregation behaviour. It is difficult to decide whether

this effect was caused by the drying method (compressed N_2), or if the crystallites are partly aggregated in dispersion.

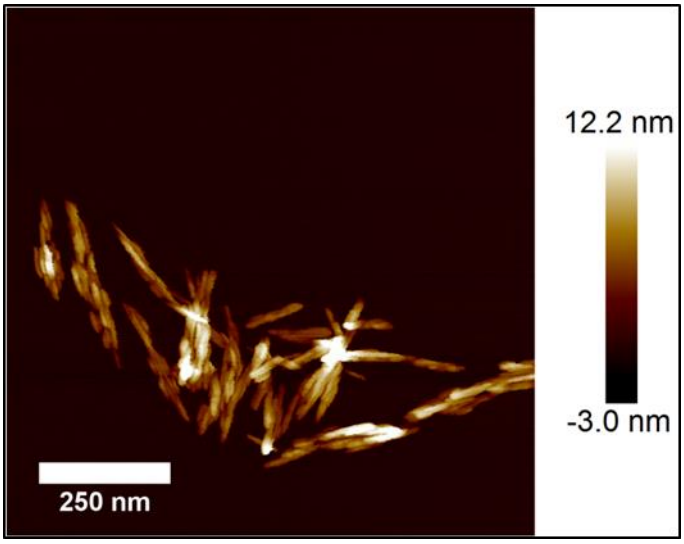

Figure 3.6: CNC crystallites dispersed in DI water and deposited onto a mica disc. The bar shown on the right indicates the height of the particles.

In Figure 3.7a-f, CNC dispersions before and after heat aging are shown. As seen, the crystallites in 3.7a and b looks quite like the non-aged crystallites in 3.6, although the sample in Fig. 3.6 is dispersed in DI-water and in Fig 3.7a in LS-brine. Nothing can be said about eventual agglomeration, as the crystallite concentration on the mica was too high. Figure 3.7c and d, shows CNC after one week of heat aging at 90 °C. Here the crystallites look changed, or spiky, which may indicate polymer degradation. This is also in agreement with the observations made through the viscosity measurements. When diluted, the crystalline particles seem to be agglomerated, as can be seen in Figure 3.7d. A CNC dispersion sample was also subjected to heat aging for one week at 120 °C, shown in Figure 3.7e and f. Here it is clear that the particles agglomerate, and this can clearly be seen in Figure 3.7e, where the agglomerates form ribbon-like structures. When diluted and magnified, as seen in Figure 3.7f,

484 large particle aggregates was observed. These observations are in accordance with the flow
485 regime seen in Figure 3.3a and b, where the crystallites are shown to flow in domains or
486 agglomerates at low shear, before breaking up at higher shear rates.

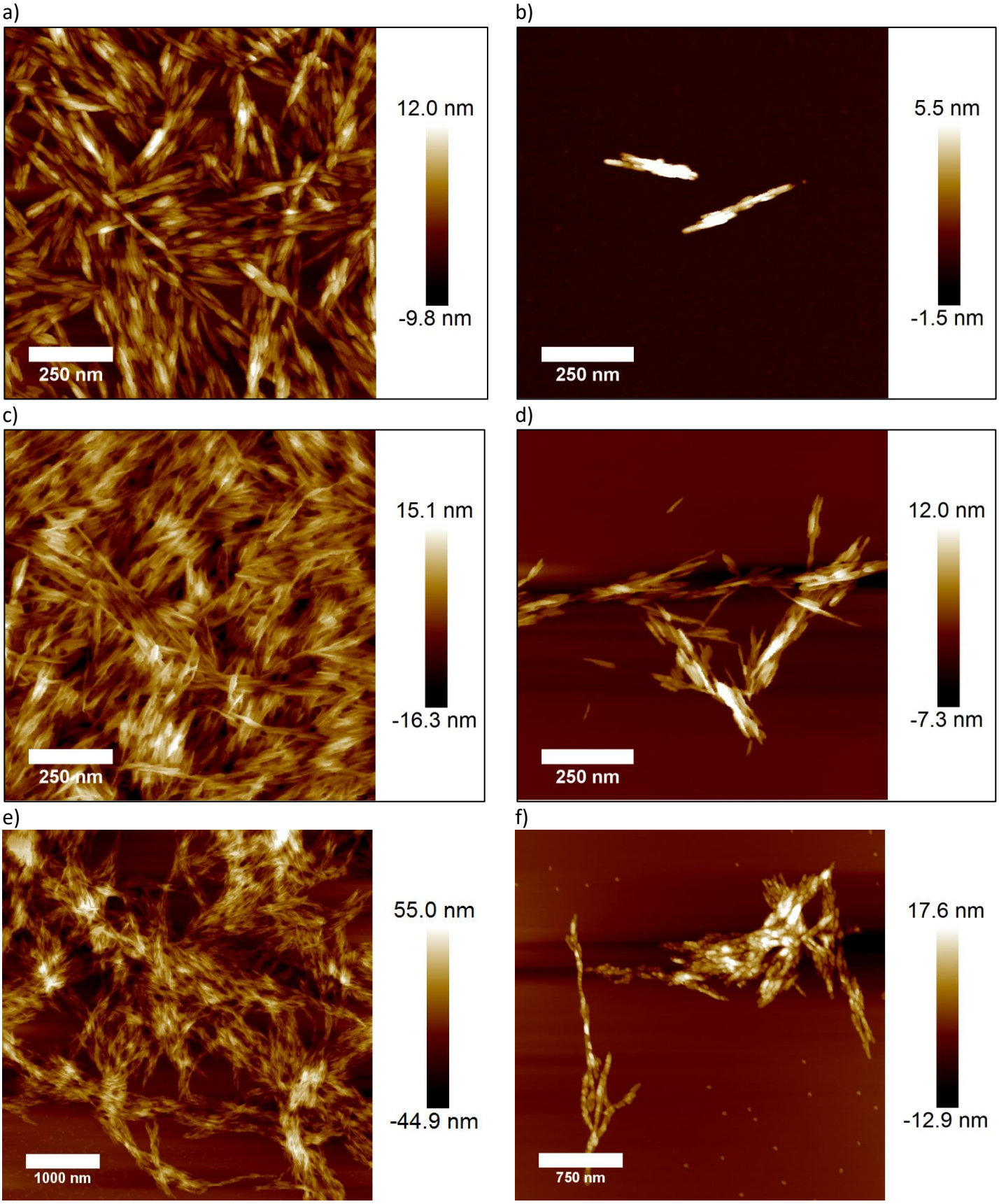

Figure 3.7: CNC before heat aging is shown in Fig a) and b). Fig c) and d) shows CNC heat aged at 90 °C for one week, while Fig e) and f) shows CNC heat aged at 120 °C for one week. The pictures on the left hand side are undiluted, and the pictures on the right hand side are diluted 10 times to show single crystallites/agglomerates.

4. Conclusions

Different types of analyses were utilised to study the stability of dispersed CNC crystallites when exposed to variations in pH, salinity and temperature. Measurements performed with Zetasizer showed that the CNC dispersion stability was not affected by either fluctuations in pH or high temperature (90 °C). These observations were supported by the viscosity measurements in the same pH range, where no significant changes in viscosity were observed with change in pH. It should be mentioned though, that the pH values tested were from slightly acidic to the basic range, for which the crystallites remained stable in dispersion. The pH values were chosen due of the intended application of the dispersions, which is enhanced oil recovery. For this type of use, the pH will never reach extreme values. A very acidic or basic environment would probably destabilise the dispersions.

For the temperature-dependent experiments, nothing definite could be concluded from the Zetasizer measurements. The zeta potential values acquired showed that the dispersions were stable for all the temperatures investigated. This is supported by the measurements done on CNC dispersions stored at 120 °C, and the shear-rest measurements performed at 90 °C. Both these testing regimens gave dispersions with increased viscosities followed by a fall and decrease in pH, where the results indicate a beginning degradation and depolymerisation of the samples. The AFM images also revealed that the crystallites are slightly agglomerated, and this tendency increases with length and temperature of heat aging.

The results shown here indicates that CNC tolerates the varying conditions it can be exposed to as a potential EOR additive, as long as it is utilised with a low salinity dispersing medium. Viscosity increase with time and temperature might be an important asset for the applicability of CNC for EOR as it may be able reduce viscous fingering and divert flow of water

in the reservoir. AFM images of particles subjected to extended heat aging also reveals that the CNC does not degrade into glucose monomers but remains crystalline within the time frame and temperatures investigated here. This type of cellulose derivate is also environmentally friendly, which is very important when introducing new chemicals for petroleum applications.

Acknowledgements

This work is performed as a part of the NORCEL Project: The NORwegian NanoCELlulose Technology Platform, initiated and led by The Paper and Fibre Research Institute (PFI) in Trondheim and funded by the Research Council of Norway through the NANO2021 Program, project number 228147. Most of the experimental work in this study has been performed at the Ugelstad Laboratory, which is part of the Department of Chemical Engineering at the Norwegian University of Science and Technology (NTNU). The AFM images in the study were acquired using instruments available at NTNU NanoLab/NorFab. The Research Council of Norway is acknowledged for the support to the Norwegian Micro- and Nano-Fabrication Facility, NorFab, project number 245963/F50.

References

Abitbol, T., et al. (2013). Estimation of the surface sulfur content of cellulose nanocrystals prepared by sulfuric acid hydrolysis. *Cellulose, 20*(2), 785-794. doi:10.1007/s10570-013-9871-0

Battista, O. A. (1950). Hydrolysis and crystallization of cellulose. *Industrial & Engineering Chemistry, 42*(3), 502-507.

Beal, C. (1946). The Viscosity of Air, Water, Natural Gas, Crude Oil and Its Associated Gases at Oil Field Temperatures and Pressures. *Transactions of the AIME 165*(1), 94-115. doi:10.2118/946094-G

Beck-Candanedo, S., et al. (2005). Effect of Reaction Conditions on the Properties and Behavior of Wood Cellulose Nanocrystal Suspensions. *Biomacromolecules, 6*(2), 1048-1054. doi:10.1021/bm049300p

Boluk, Y., et al. (2011). Suspension viscosities and shape parameter of cellulose nanocrystals (CNC). *Colloids and Surfaces A: Physicochemical and Engineering Aspects, 377*(1–3), 297-303. doi:http://dx.doi.org/10.1016/j.colsurfa.2011.01.003

Camarero Espinosa, S., et al. (2013). Isolation of thermally stable cellulose nanocrystals by phosphoric acid hydrolysis. *Biomacromolecules, 14*(4), 1223-1230.

Chen, L., et al. (2016). Highly thermal-stable and functional cellulose nanocrystals and nanofibrils produced using fully recyclable organic acids. *Green Chemistry*.

de Souza Lima, M. M., & Borsali, R. (2004). Rodlike cellulose microcrystals: structure, properties, and applications. *Macromolecular Rapid Communications, 25*(7), 771-787.

Dong, X. M., et al. (1996). Effects of ionic strength on the isotropic-chiral nematic phase transition of suspensions of cellulose crystallites. *Langmuir, 12*(8), 2076-2082.

Dunlop, A. (1948). Furfural formation and behavior. *Industrial & Engineering Chemistry, 40*(2), 204-209.

Gray, D., & Rex, R. (1965). *Formation damage in sandstones caused by clay dispersion and migration.* Paper presented at the Proc.

Habibi, Y., et al. (2010). Cellulose nanocrystals: chemistry, self-assembly, and applications. *Chemical Reviews, 110*(6), 3479-3500.

Heggset, E. B., et al. (2017). Temperature stability of nanocellulose dispersions. *Carbohydrate Polymers, 157*, 114-121. doi:http://dx.doi.org/10.1016/j.carbpol.2016.09.077

Jahn, F., et al. (2008). Exploration *Hydrocarbon Exploration and Production* (2nd ed., pp. 21-22). Amsterdam: Elsevier.

Julien, S., et al. (1993). Influence of acid pretreatment (H2SO4, HCl, HNO3) on reaction selectivity in the vacuum pyrolysis of cellulose. *Journal of Analytical and Applied Pyrolysis, 27*(1), 25-43. doi:http://dx.doi.org/10.1016/0165-2370(93)80020-Z

Klemm, D., et al. (2011). Nanocelluloses: A New Family of Nature-Based Materials. *Angewandte Chemie International Edition, 50*(24), 5438-5466. doi:10.1002/anie.201001273

Lahiji, R. R., et al. (2010). Atomic Force Microscopy Characterization of Cellulose Nanocrystals. *Langmuir, 26*(6), 4480-4488. doi:10.1021/la903111j

Leong, Y., & Ong, B. (2003). Critical zeta potential and the Hamaker constant of oxides in water. *Powder Technology, 134*(3), 249-254.

Liao, C.-H., et al. (2001). Hydroxyl radical scavenging role of chloride and bicarbonate ions in the H2O2/UV process. *Chemosphere, 44*(5), 1193-1200. doi:http://dx.doi.org/10.1016/S0045-6535(00)00278-2

Łojewska, J., et al. (2007). Carbonyl groups development on degraded cellulose. Correlation between spectroscopic and chemical results. *Applied Physics A, 89*(4), 883-887.

576 Lu, M.-C., et al. (2005). Effect of chloride ions on the oxidation of aniline by Fenton's reagent. *Journal*
577 *of Environmental Management, 75*(2), 177-182.
578 doi:http://dx.doi.org/10.1016/j.jenvman.2004.12.003
579 Marchessault, R., et al. (1961). Some hydrodynamic properties of neutral suspensions of cellulose
580 crystallites as related to size and shape. *Journal of Colloid Science, 16*(4), 327-344.
581 Matsuo, M., et al. (2012). Kinetic analysis of color changes in cellulose during heat treatment. *Journal*
582 *of wood science, 58*(2), 113-119.
583 Molnes, S., et al. (2016). Sandstone injectivity and salt stability of cellulose nanocrystals (CNC)
584 dispersions—Premises for use of CNC in enhanced oil recovery. *Industrial Crops and Products,*
585 *93*, 152-160. doi:http://dx.doi.org/10.1016/j.indcrop.2016.03.019
586 Orts, W., et al. (1998). Enhanced ordering of liquid crystalline suspensions of cellulose microfibrils: A
587 small angle neutron scattering study. *Macromolecules, 31*(17), 5717-5725.
588 Payen, A. (1838). Mémoire sur la composition du tissu propre des plantes et du ligneux. *Comptes*
589 *rendus, 7*, 1052-1056.
590 Roman, M., & Winter, W. T. (2004). Effect of Sulfate Groups from Sulfuric Acid Hydrolysis on the
591 Thermal Degradation Behavior of Bacterial Cellulose. *Biomacromolecules, 5*(5), 1671-1677.
592 doi:10.1021/bm034519+
593 Rånby, B. G. (1949). Aqueous colloidal solutions of cellulose micelles. *Acta Chemica Scandinavia, 3*(5),
594 649-650. doi:DOI number: 10.3891/acta.chem.scand.03-0649
595 Sacui, I. A., et al. (2014). Comparison of the properties of cellulose nanocrystals and cellulose
596 nanofibrils isolated from bacteria, tunicate, and wood processed using acid, enzymatic,
597 mechanical, and oxidative methods. *ACS applied materials & interfaces, 6*(9), 6127-6138.
598 Salopek, B., et al. (1992). *Measurement and application of zeta-potential*: Rudarsko-geološko-naftni
599 fakultet.
600 Sarkar, P., & Nicholson, P. S. (1996). Electrophoretic deposition (EPD): mechanisms, kinetics, and
601 application to ceramics. *Journal of the American Ceramic Society, 79*(8), 1987-2002.
602 Shen, D., et al. (2013). The overview of thermal decomposition of cellulose in lignocellulosic biomass
603 *Cellulose-Biomass Conversion*: InTech.
604 Skauge, T., et al. (2010). *Nano-sized particles for EOR.* Paper presented at the SPE Improved Oil
605 Recovery Symposium.
606 Wang, N., et al. (2007). Thermal degradation behaviors of spherical cellulose nanocrystals with sulfate
607 groups. *Polymer, 48*(12), 3486-3493. doi:http://dx.doi.org/10.1016/j.polymer.2007.03.062
608 Wang, S. C., & Wei, W. C. J. (2001). Electrokinetic properties of nanosized SiC particles in highly
609 concentrated electrolyte solutions. *Journal of the American Ceramic Society, 84*(7), 1411-
610 1414.
611 Wellington, S. L. (1983). Biopolymer solution viscosity stabilization-polymer degradation and
612 antioxidant use. *Society of petroleum engineers journal, 23*(06), 901-912.
613 Will, J., et al. (2001). Electrophoretic deposition of zirconia on porous anodic substrates. *Journal of the*
614 *American Ceramic Society, 84*(2), 328-332.
615 Yatagai, M., & Zeronian, S. (1994). Effect of ultraviolet light and heat on the properties of cotton
616 cellulose. *Cellulose, 1*(3), 205-214.

617